Cell Reports
Article

Ion Channel Profile of TRPM8 Cold Receptors Reveals a Role of TASK-3 Potassium Channels in Thermosensation

Cruz Morenilla-Palao,[1,*] Enoch Luis,[1] Carlos Fernández-Peña,[1] Eva Quintero,[1] Janelle L. Weaver,[2] Douglas A. Bayliss,[2] and Félix Viana[1,*]
[1]Instituto de Neurociencias de Alicante, Universidad Miguel Hernández-CSIC, 03550 San Juan de Alicante, Spain
[2]Department of Pharmacology, University of Virginia, Charlottesville, VA 22908, USA
*Correspondence: cruz@umh.es (C.M.-P.), felix.viana@umh.es (F.V.)
http://dx.doi.org/10.1016/j.celrep.2014.08.003

SUMMARY

Animals sense cold ambient temperatures through the activation of peripheral thermoreceptors that express TRPM8, a cold- and menthol-activated ion channel. These receptors can discriminate a very wide range of temperatures from innocuous to noxious. The molecular mechanism responsible for the variable sensitivity of individual cold receptors to temperature is unclear. To address this question, we performed a detailed ion channel expression analysis of cold-sensitive neurons, combining bacterial artificial chromosome (BAC) transgenesis with a molecular-profiling approach in fluorescence-activated cell sorting (FACS)-purified TRPM8 neurons. We found that TASK-3 leak potassium channels are highly enriched in a subpopulation of these sensory neurons. The thermal threshold of TRPM8 cold neurons is decreased during TASK-3 blockade and in mice lacking TASK-3, and, most importantly, these mice display hypersensitivity to cold. Our results demonstrate a role of TASK-3 channels in thermosensation, showing that a channel-based combinatorial strategy in TRPM8 cold thermoreceptors leads to molecular specialization and functional diversity.

INTRODUCTION

The ability to transduce specific sensory stimuli by molecularly defined subpopulations of primary sensory afferents has emerged as a fundamental aspect in the organization of the somatosensory system (reviewed by Belmonte and Viana, 2008; Lumpkin and Caterina, 2007). The trigeminal and dorsal root ganglia (TG and DRG, respectively) contain distinct subpopulations of primary sensory neurons, categorized according to several morphological and functional criteria, including the threshold response to an adequate stimulus (e.g., temperature, mechanical, and chemical) (Scott, 1992). These neurons are thought to establish dedicated sensory lines (i.e., labeled lines), carrying information from the periphery to the CNS that finally results in the perception of temperature, touch, itch, and pain (Ma, 2010).

The discrimination between warm and cold temperatures, and innocuous (i.e., mild) versus a potentially damaging noxious thermal stimulus, depends also on the activity of specific subpopulations of primary sensory afferents (reviewed by Belmonte et al., 2009; Foulkes and Wood, 2007). Ion channels of the transient receptor potential (TRP) family play a critical role as molecular sensors of ambient stimuli (Bandell et al., 2007; Clapham, 2003). A subpopulation of thermoreceptors expresses TRPM8, a cold- and menthol-activated ion channel, known to play a critical role in cold sensation (Bautista et al., 2007; Colburn et al., 2007; Dhaka et al., 2007; Pogorzala et al., 2013). In heterologous expression systems, the activation of TRPM8 occurs in a narrow temperature range, with a mean around 25°C. In contrast, cold-sensitive neurons expressing TRPM8 show a very wide range of temperature thresholds (reviewed by Almaraz et al., 2014), suggesting that cold sensitivity of sensory neurons might be tuned by other molecular entities. Although initial studies suggested that TRPM8 expression defines a relatively uniform population of low-threshold cold thermoreceptors, subsequent work revealed important differences in their neurochemical content, peripheral innervation targets, and cold sensitivity (Dhaka et al., 2008; Takashima et al., 2007; Xing et al., 2006). Indeed, several lines of evidence support a fundamental role of TRPM8-expressing neurons in both innocuous and noxious cold detection (Almaraz et al., 2014; Julius, 2013; Knowlton et al., 2013). Therefore, a current challenge in the field of cold thermoreception is to understand how a single molecular temperature sensor (i.e., TRPM8) might operate over such a wide temperature range. A favored hypothesis argues that variable coexpression of TRPM8 with other ion channels, like potassium (K^+) selective channels, adjusts the thermal sensitivity of individual thermoreceptors (Madrid et al., 2009; Noël et al., 2009).

To shed light on this question, we have defined the ion "channelome" of TRPM8 peripheral sensory neurons by using bacterial artificial chromosome (BAC) transgenesis to genetically label neurons expressing the molecular cold sensor TRPM8. We combined this approach with gene expression analysis in TRPM8 neurons purified by fluorescence-activated cell sorting (FACS). This molecular profiling revealed an unexpected enrichment of several ion channels in cold thermoreceptors. In particular, we found that TASK-3, a pH-sensitive two-pore domain leak K^+

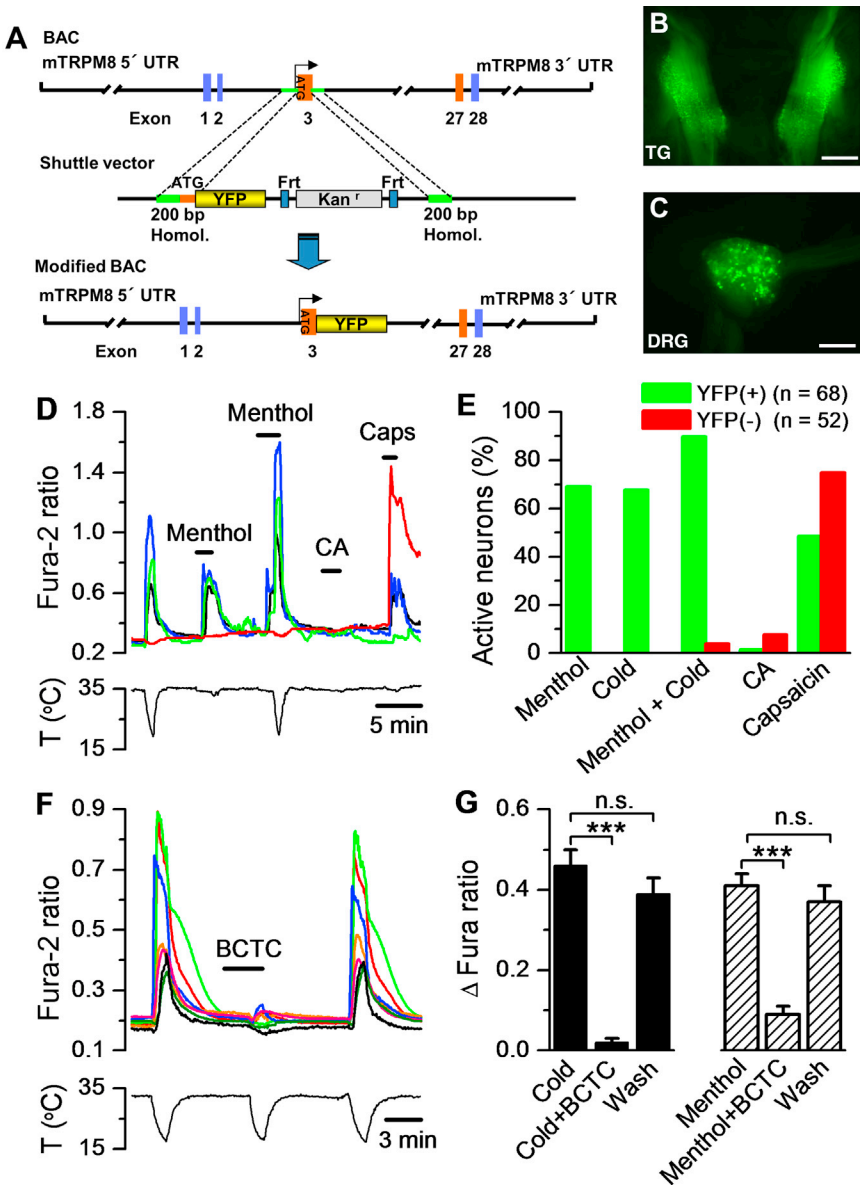

Figure 1. Generation and Characterization of TRPM8^{BAC}-EYFP Transgenic Mouse Line

(A) Targeting strategy to obtain a BAC containing the EYFP gene under the direction of regulatory elements from the mouse TRPM8 gene.

(B and C) Fluorescent expression in the TG and DRG of the TRPM8^{BAC}-EYFP transgenic mouse line in fresh tissue. Scale bars represent 1 mm.

(D) Fura-2 traces of FACS-purified EYFP-labeled neurons challenged with cold, menthol (100 μM), cold plus menthol, cinnamaldeheyde (CA; 100 μM), and capsaicin (100 nM).

(E) Quantification of neurons responding to each stimulus (as percentage of total) in EYFP^{+} (green) and EYFP^{-} (red) neurons.

(F) Effect of BCTC (10 μM) on cold-evoked responses in ten fluorescence-activated cell-sorted EYFP^{+} neurons recorded simultaneously.

(G) Histogram of BCTC (10 μM) block of cold- and menthol-evoked responses in sorted YFP^{+} neurons (n = 24) from TRPM8^{BAC}-EYFP$^{+/-}$ mice. Values are mean ± SEM. ***p < 0.001, one-way ANOVA and Dunnett posttest. n.s., not significant.

RESULTS

Genetically Labeled Sensory Neurons of TRPM8^{BAC}-EYFP Mice Are Cold and Menthol Sensitive

To identify sensory neurons expressing the TRPM8 channel in vivo, we used a genetic strategy. A BAC containing the entire mouse TRPM8 locus was modified by inserting the cDNA encoding for the enhanced yellow fluorescent protein (EYFP) in frame after the Met10 of TRPM8 (Figure 1A). Eight different founder lines were obtained. All TRPM8^{BAC}-EYFP$^{+/-}$ transgenic mice showed an intense fluorescence in a fraction of cell bodies in peripheral sensory ganglia that could be visualized in fresh, living tissue under a fluorescence microscope (Figures 1B and 1C). EYFP immunostaining was detected in all tissues where targeting of cold sensory neurons expressing TRPM8 channels has been described, including the superficial dorsal horn of the spinal cord, where DRG afferent sensory neurons terminate, in trigeminal corneal terminals, and in sensory lingual fibers surrounding taste buds in the tongue (Abe et al., 2005; Dhaka et al., 2008; Parra et al., 2010; Takashima et al., 2007) (Figures S1A–S1C). In agreement with the early developmental expression of TRPM8, intense fluorescence was also observed in sensory ganglia and peripheral tissues of embryonic mice (Figure S1D).

Mean neuronal diameter of EYFP-labeled neurons was 18.6 ± 0.4 μm (Figure S1E), consistent with the expression of TRPM8 in small-to-medium-sized sensory neurons (Dhaka et al., 2008; McKemy et al., 2002; Peier et al., 2002a; Takashima et al., 2007). In fact, we observed two different types of fluorescent channel (Duprat et al., 1997; Kim et al., 2000), is enriched about 140-fold in TRPM8 neurons, and it is expressed in a specific subpopulation of these thermoreceptors. Functional studies on TRPM8-expressing neurons from TASK-3 knockout (TASK-3^{KO}) mice showed that high-threshold TRPM8 cold neurons are absent in these animals and revealed an overall shift of their thermal threshold toward warmer temperatures in the absence of TASK-3. Consistent with this finding, TASK-3^{KO} mice are more sensitive to cold stimuli in behavioral assays. Our strategy offers the opportunity to explore the unique role of specific ion channels in cold transduction and cold pain and provides detailed ion channel expression profile of peripheral cold thermoreceptors. These results demonstrate that peripheral thermosensory neurons can fine-tune their excitability to sensory stimuli by the combinatorial expression of specific ion channels.

neurons: a small diameter neuronal population with strong EYFP expression and a second population of medium-to-large diameter neurons with fainter EYFP expression; the last group is more obvious when the signal is amplified by antiyellow fluorescent protein (anti-YFP) immunostaining. As a further characterization of TRPM8^{BAC}-EYFP$^{+/-}$ mice, we assessed the expression of different neuronal markers in EYFP^{+} cells from DRG sections, which revealed the near absence of IB4 label (Figures S1F and S1G).

To examine the sensory phenotype of EYFP-expressing neurons, we performed calcium (Ca^{2+}) imaging on DRG cultures from TRPM8^{BAC}-EYFP$^{+/-}$ mice, testing the effects of cold and menthol, canonical agonists of TRPM8 (McKemy et al., 2002; Peier et al., 2002a). As predicted, the majority (52 of 58 [90%]) of EYFP-labeled neurons responded to both stimuli (Figure S2A) and showed different activation thresholds for the cooling stimulus, confirming that they express TRPM8 and behave as bona fide TRPM8-expressing neurons. Importantly, almost none of the EYFP^{-} neurons responded to cold and menthol (1.5%, n = 327; $p < 0.0001$, Fisher's exact test) (Figure S2B), further demonstrating that the EYFP-labeled neurons from TRPM8^{BAC}-EYFP$^{+/-}$ mice faithfully recapitulate the sensory characteristics that define TRPM8-expressing sensory neurons in wild-type (WT) mice.

To decipher the selective channel expression profile of TRPM8 cold receptors, we isolated a purified population of these neurons from the entire sensory ganglia by FACS. First, we analyzed a DRG cell suspension from WT mice to set up the optimal conditions for single-cell sorting and as a negative control for fluorescence detection (Figure S3A, top panels). A cell suspension from TRPM8^{BAC}-EYFP$^{+/-}$ transgenic mice was then analyzed, and a cellular population expressing EYFP was detected, sorted, and cultured, achieving a purity of 85%–90% (based on the ratio of fluorescent versus nonfluorescent cells) with high levels of survival (Figures S3A, bottom panels, and S3B). Functional studies on these FACS-enriched EYFP-expressing cultures showed that 24 hr after seeding, cultured sensory neurons maintained their ability to respond to menthol and cold, demonstrating that the sorting process did not affect their functional properties (Figure 1D). Altogether, 69.1% (47 of 68) of EYFP-sorted neurons responded to a cold stimulus, and 67.7% (46 of 68) also responded to menthol (100 μM) application. Coapplication of menthol during a cooling stimulus, a more potent activator of TRPM8, increased the number of responses in EYFP^{+} neurons to 89.7% (61 of 68). In line with previous studies, we found that about half of the menthol- and cold-sensitive EYFP neurons (48%, 33 of 68) also responded to the application of capsaicin (100 nM) (Figure 1E), demonstrating the coexpression in the same neuron of the vanilloid receptor TRPV1. In contrast, EYFP^{+} neurons did not respond (1.5%, 1 of 68) to the specific TRPA1 agonist cinnamaldehyde (CA), confirming that TRPA1 channels are not coexpressed in TRPM8 neurons (Pogorzala et al., 2013; Story et al., 2003). We found no difference in mean temperature threshold values between sorted (28.0°C ± 0.4°C; n = 50) and nonsorted (28.8°C ± 0.3°C; n = 46) cultured EYFP^{+} neurons ($p = 0.065$, unpaired t test). Moreover, cold and menthol responses were significantly and reversibly blocked by 4-(3-chloro-pyridin-2-yl)-piperazine-1-carboxylic acid (4-tert-butyl-phenyl)-amide (BCTC) (10 μM) (Figures 1F and 1G), an antagonist of TRPM8 channels (Madrid et al., 2006). Altogether, these results demonstrate that EYFP-labeled neurons from TRPM8^{BAC}-EYFP$^{+/-}$ mice recapitulate the same cellular and sensory properties that define TRPM8-expressing sensory neurons in WT mice, and validate our genetic strategy for the in vivo labeling of cold thermoreceptors. Also, these results show that by using FACS, we are able to obtain a highly enriched population of healthy and fully functional cold sensory neurons that express the TRPM8 ion channel.

Ion Channel Expression Analysis of TRPM8 Cold Sensory Neurons

The coexpression of other voltage-gated ion channels in TRPM8-expressing cold thermoreceptors has a major impact on their excitability (Madrid et al., 2009; Vetter et al., 2013) and their discharge pattern (Orio et al., 2009, 2012), shaping their transduction and encoding properties. Thus, the quantitative characterization of the full complement of ion channels expressed in TRPM8 neurons would be a key step to reveal regulators of their excitability, an important question in the pathophysiology of cold pain (reviewed by Belmonte et al., 2009). To define the ion channel profile of TRPM8 cold sensory neurons, we used a customized TaqMan low-density array that included many ion channels and receptors known to be expressed in sensory neurons. The full list of ion channels and receptors examined in our study is indicated in Table S1. FACS-based purification of TRPM8-expressing neurons from DRGs of TRPM8^{BAC}-EYFP$^{+/-}$ mice was performed, and the mRNA was extracted and copied to cDNA. As a reference, we also recovered the population of sorted neurons not expressing TRPM8 because it represents the gene expression pattern of a heterogeneous pool of unlabeled sensory neurons. A clearly differentiated ion channel expression profile was obtained for TRPM8 sensory neurons versus non-TRPM8 neurons (Figure 2A; Table S1). Importantly, the mRNA for TRPM8 was enriched about 700 times in the population of fluorescent cells (Figures 2A and 2B), confirming the purity of the samples.

In addition to TRPM8, several other ion channels were differentially expressed in these neurons (Figures 2B and 2C). Most interestingly, TRPM8 neurons are characterized by very high expression of the two-pore domain potassium channel TASK-3 (Kcnk9), which is enriched around 140 times (140.7 ± 13.4-fold expression; n = 3). High ratios were also found for the amiloride-sensitive channel subunit Asic4 (Accn4) (26.6 ± 6.6-fold expression; n = 3) and the calcium-activated potassium channel SK3 (Kcnn3) (17.9 ± 2.0-fold expression; n = 3). By contrast, other channels such as TRPC6 and TRPA1, or the Mrgprd receptor, showed a very low relative expression in TRPM8 neurons (Figure 2B; Table S1). The mRNA for Kir3.4 (kcnj5) and TRPV3 was not detected in either of the two populations assayed (Table S1).

To confirm the results obtained with the TaqMan array, we tested the expression of several ion channels (TASK-3 [Kcnk9], SK3 [Kcnn3], TREK-1 [Kcnk2], GIRK3 [Kcnj9], and Asic2 [Accn2]), with different levels of enrichment in TRPM8 neurons, by an independent quantitative RT-PCR (RT-qPCR) analysis. In all cases, the relative expression for all the channels was fully

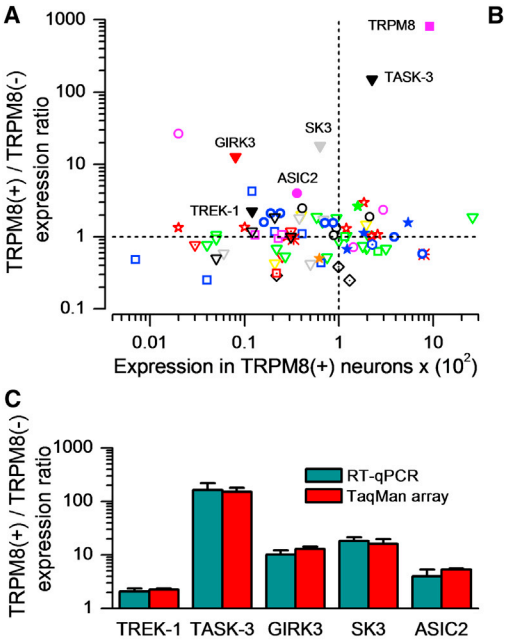

B

KEY	GENE	TRPM8(+)/TRPM8(-)	p value
■	TRPM8	729,40	7,77E-05
▼	KCNK9 / TASK-3	140,71	2,16E-04
○	ACCN4	26,60	1,10E-02
▽	KCNN3 / SK3	17,88	4,62E-04
▼	KCNJ9 / GIRK3	13,19	1,48E-02
□	TRPC2	4,35	2,08E-02
●	ACCN2 / ASIC2	3,95	5,48E-03
★	TH	2,65	9,60E-03
○	HCN4	2,46	4,23E-04
○	ACCN3	2,39	1,80E-02
▽	KCNK2	2,23	6,26E-03
○	SCN3A	2,07	4,28E-03
○	SCN5A	2,09	2,38E-03
▽	KCNMB2	1,97	7,50E-03
○	HCN1	1,87	2,41E-03
▽	KCNC2	1,85	1,64E-02
▽	KCNAB2	1,85	1,16E-02
▽	KCNC1	1,83	7,07E-03
▽	KCNN2	1,81	3,15E-02
▽	KCNJ4	1,73	2,00E-02
▽	KCNQ2	1,73	1,10E-02
○	SCN2A1	1,60	4,00E-02
★	NTRK1	1,57	1,04E-02
▽	KCNMA1	1,44	5,29E-02
○	HCN2	1,34	1,53E-02
▽	KCND3	0,74	4,10E-02
▽	KCNA6	0,71	1,27E-02
▽	KCND1	0,68	3,10E-02
★	NTRK2	0,68	3,51E-04
▽	KCNN4	0,59	2,27E-02
○	SCN10A	0,59	2,76E-02
✱	P2RX3	0,58	3,68E-02
▽	KCNJ10	0,53	1,87E-03
▽	KCNA1	0,53	9,30E-03
▽	KCNAB1	0,52	3,15E-02
▽	KCNK5	0,51	5,41E-03
★	CACNA1I	0,48	5,14E-03
□	TRPC5	0,46	3,80E-02
○	SCN11A	0,44	1,09E-02
□	TRPC3	0,44	1,02E-02
▽	KCNMB1	0,42	8,51E-03
▽	KCNN1	0,43	1,68E-03
◇	MRGPRX1	0,37	2,41E-03
□	TRPA1	0,31	1,54E-02
◇	MRGPRD	0,26	6,00E-04
□	TRPC6	0,25	1,14E-02

Figure 2. Ion Channel Expression Profile of TRPM8 Sensory Neurons

(A) 2D representation in logarithmic scale of TaqMan array mean expression values (n = 3), showing normalized differential expression of ion channels in TRPM8(+) versus TRPM8(−) neurons (y axis) and relative expression of different ion channels in TRPM8(+) neurons normalized to glyceraldehyde 3-phosphate dehydrogenase (x axis). The symbols correspond to different families of ion channels and receptors as shown in (B).

(B) Table showing the most differentially expressed ion channels, comparing TRPM8(+) to TRPM8(−) neurons and their respective p values (n = 3). For some gene products, alternative nomenclature is shown.

(C) Comparison of expression levels (mean ± SEM) of selected ion channels (labeled in A) in fluorescence-activated cell-sorted TRPM8(+) neurons obtained by RT-qPCR expression and TaqMan array probes (n = 3).

consistent with the results of our previous TaqMan experiment (Figure 2C).

We also investigated whether the expression of TASK-3 and SK3 (two of the channels most enriched in TRPM8 neurons) colocalized in TRPM8 neurons at the protein level on DRG sections from TRPM8^{BAC}-EYFP$^{+/-}$ mice. As shown in Figure 3A, TASK-3 and SK3 channels colocalized significantly with a fraction of TRPM8^{+} neurons. From the total of TRPM8 neurons, 33.6% ± 2.5% were TASK-3 positive, and 45.6% ± 5.2% were positive for SK3 (Figure 3B). On the other hand, about 68% of the TASK-3-positive neurons and 73% of SK3-positive neurons were positive for TRPM8. These results indicate that there are different subpopulations of TRPM8 cold neurons with specific ion channel expression profiles, being one of these populations highly enriched in TASK-3 channels.

TRPM8 Sensory Neurons Express a TASK-3-like Current

Next, we sought to examine the functionality of TASK-3 in TRPM8 cold neurons. To this end, we generated a transgenic mouse line from the TRPM8^{BAC}-EYFP$^{+/-}$, the TASK-3^{KO}: TRPM8^{BAC}-EYFP$^{+/-}$, which provided EYFP-labeled TRPM8 sensory neurons that were also deleted for TASK-3. For simplicity, we will call them WT and TASK-3^{KO}, respectively.

TASK-3 is a member of the large subfamily of two-pore domain potassium (K2P) channels (Kim et al., 2000; Lesage and Barhanin, 2011). These channels give rise to voltage-independent, leak K^+ currents, which contribute to the resting membrane potential and input resistance and thereby regulate neuronal excitability. The conductance of TASK-1/TASK-3 channels is decreased by extracellular acidification (Duprat et al., 1997; Talley and Bayliss, 2002). Therefore, we investigated the effect of low pH (6.0) on whole-cell currents in TRPM8 neurons. The membrane potential was held at −20 mV, and voltage ramps to −120 mV were applied every 10 s. To minimize potential effects of pH on prominent hyperpolarization-activated (Ih) currents, we applied 1 mM Cs^+ beforehand. Low pH produced a reversible reduction of the standing whole-cell outward current at −20 mV of 74.8 ± 14.4 pA, representing 49.9% ± 3.2% of the total current at this potential (n = 6) (Figures 4A and 4B). Shown in Figure 4D is the mean current density at −20 mV in control (pH 7.4) and acidic (pH 6.0) solution. The pH-sensitive current was outwardly rectifying, reversed at −80.7 ± 2.5 mV (n = 6), and was well fitted by a Goldman-Hodgkin-Katz (GHK) equation (Figure 4C), thus sharing biophysical properties of K^+-selective currents. In TRPM8 neurons from TASK-3^{KO} mice, the current density at pH 7.4, measured at −20 mV, was reduced to about half compared to WT (10.6 ± 1.4 pA/pF versus 4.5 ± 0.6 pA/pF; $p < 0.01$) (Figures 4E and 4F). A fraction of this current was also sensitive to low pH, outwardly rectifying, and with a reversal potential of −90.2 ± 4.5 mV (n = 6). The density of the pH-sensitive current was also significantly smaller in TASK-3^{KO} neurons compared to WT (5.3 ± 0.8 pA/pF versus 2.9 ± 0.4 pA/pF; $p < 0.05$, unpaired t test) (Figure 4F). This result indicates that about 45% of the total pH-sensitive current in TRPM8^{+} neurons can be attributed to TASK-3. The remaining pH-sensitive current could be carried by TASK-1, widely expressed in DRG neurons (Talley et al., 2001). In contrast, the whole-cell capacitance and the amplitude of the Ih were not significantly different between WT and TASK-3^{KO} neurons (data not shown), ruling out general, nonspecific effects of TASK-3 deletion on the electrophysiological properties of TRPM8 neurons.

The arsenal of specific TASK-3 channel inhibitors is currently very limited (Lesage and Barhanin, 2011). The divalent cation Zn^{2+} can discriminate between TASK-1 and TASK-3 channels, blocking the latter with greater potency (Clarke et al., 2004). We used Ca^{2+} imaging to test the effects of Zn^{2+} on cultured DRG neurons. As shown in Figure S4A, 100 μM Zn^{2+} activated TRPM8 and non-TRPM8 neurons. However, activation of TRPM8-expressing neurons was much more likely, occurring

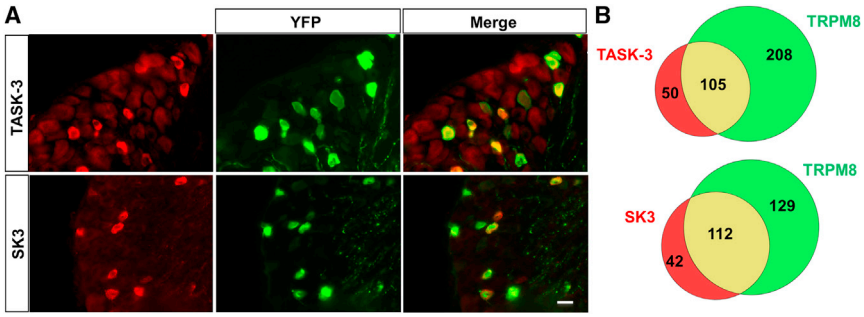

Figure 3. TASK-3 and SK3 Are Highly Expressed in TRPM8 Neurons

(A) Immunostaining of DRG sections from TRPM8^{BAC}-EYFP$^{+/-}$ mice with anti-TASK-3 and anti-SK3. Scale bar represents 20 μm.

(B) Venn diagrams showing the relative size and overlap between the population of TRPM8(+) neurons and TASK-3 or SK3 immunoreactivity in DRG sections of 1- to 2-month-old mice.

in 28 of 61 neurons compared to only 43 of 364 TRPM8$^-$ neurons ($p < 0.001$, Fisher's exact test) (Figure S4B). The potent effects of Zn^{2+} on some TRPM8$^-$ neurons correlated with their CA sensitivity (Figures S4A and S4C) and are likely due to activation of TRPA1 channels by Zn^{2+} (Andersson et al., 2009; Hu et al., 2009). Moreover, the excitatory effects of Zn^{2+} on TRPM8 neurons cannot be explained by direct excitatory effects on TRPM8 channels because Zn^{2+} had a clear blocking effect on cold-induced increases of intracellular Ca^{2+} in human embryonic kidney 293 (HEK293) cells expressing TRPM8 (Figures S4D–S4F).

Recently, a specific inhibitor, a 5,6,7,8-tetrahydropyrido[4,3-d] pyrimidine analog, was described for recombinant human TASK-3 channels, with a 10-fold potency over TASK-1 (Coburn et al., 2012). We tested the effect of this drug, known as compound 23 (C23), on mouse TASK-3 channels overexpressed in HEK293 cells. As shown in Figures 5A–5C, 200 nM C23 inhibited 84.0% ± 1.5% of the whole-cell current at 0 mV in a reversible manner. The C23-sensitive currents were outwardly rectifying and reversed at −95.0 ± 2.6 mV (n = 5). At 1 μM, the block was nearly complete and equivalent to the inhibition produced by pH 6.0. Next, we examined the effect of C23 on the thermal sensitivity of TRPM8 neurons. At 1 μM, C23 produced a reversible shift in their temperature-activation threshold during a cooling pulse (Figures 5D and 5E). This shift was observed in 13 of 32 neurons tested, which is a very similar percentage of TRPM8 neurons activated by Zn^{2+}. On average, mean threshold shifted from 28.7°C ± 0.5°C in control to 30.6°C ± 0.3°C in the presence of C23 ($p < 0.001$; n = 13) (Figure 5F). Collectively, these results demonstrate the expression of a TASK-3 current in TRPM8 neurons and its influence on cold sensitivity.

Cold Sensitivity of TRPM8 Sensory Neurons Is Altered in TASK-3^{KO} Mice

Some members of the K2P channel family (TREK-1, TREK-2, and TRAAK) are very sensitive to temperature (Kang et al., 2005; Maingret et al., 2000) and are thought to play important roles in modulating the excitability of primary sensory neurons (Noël et al., 2009). In fact, closure of leak K^+ channels has been proposed as an alternative mechanism of cold temperature transduction in peripheral (Reid and Flonta, 2001; Viana et al., 2002) and central neurons (de la Peña et al., 2012).

A previous study showed that TASK-3 channels have very modest temperature sensitivity (Kang et al., 2005; Kim et al., 2000). We confirmed that mouse TASK-3 currents are minimally affected in a temperature range from 20°C to 33°C (Figure S5). In contrast, the amplitude of mouse TREK-1 currents increased more than 10-fold in the same temperature range (Figure S5).

Next, to investigate the possible role of TASK-3 channels in cold temperature sensing, we studied the effect of low-temperature pulses on TRPM8 neurons from WT and TASK-3^{KO} mice. First, we verified that TASK-3 deletion in TASK-3^{KO} mice did not alter TRPM8 channel expression in DRG neurons (Figure S6). Next, YFP-labeled neurons were isolated by FACS, and their responses to cold and menthol stimuli were characterized by Ca^{2+} imaging. As shown in Figures 6A and 6B, these neurons retained their responsiveness to both cold and menthol. Indeed, the amplitude of Ca^{2+} responses was significantly enhanced when compared to responses obtained in the same neurons sorted from WT mice (Figure 6A). Moreover, the application of individual agonists of TRPM8 (i.e., cold or menthol) produced a nearly full recruitment of EYFP-labeled neurons in TASK-3^{KO} mice, whereas responses to CA or capsaicin were unaffected (Figure 6B). Finally, we assessed the temperature threshold of TRPM8 neurons in animals lacking TASK-3. As shown in Figure 6C, we found a significant shift in the mean threshold toward warmer temperatures in TASK-3^{KO} cold-sensitive neurons (28.0°C ± 0.4°C in WT [n = 46] versus 29.9°C ± 0.2°C in the TASK-3^{KO} [n = 68]; $p < 0.001$, unpaired t test). This overall shift in mean threshold value in TASK-3^{KO} DRG neurons was due primarily to a strong reduction in the high-threshold population of cold neurons. Altogether, our results suggest that sensitivity of TRPM8 sensory neurons to agonists is enhanced in the absence of TASK-3, and coexpression of the TASK-3 channel with TRPM8 acts as a brake in excitability, dampening the sensitivity to the cold temperature of high-threshold cold neurons.

Excitability of TRPM8-Expressing Sensory Neurons Is Augmented in TASK-3^{KO} Mice

Because TASK-3 is involved in setting the resting membrane potential and the excitability of peripheral and central neurons (Plant, 2012; Talley et al., 2001), we examined electrophysiological properties of TRPM8 neurons in WT mice and TASK-3^{KO} mice. In both groups of animals, the overall electrophysiological properties of EYFP-labeled neurons were typical for cold- and menthol-activated primary sensory neurons (Reid et al., 2002; Viana et al., 2002). These neurons are characterized by rapid regular firing, strong sag and rebound discharge during hyperpolarizing pulses, and short duration action potentials (Figures S7A–S7C). The resting membrane potential was depolarized almost

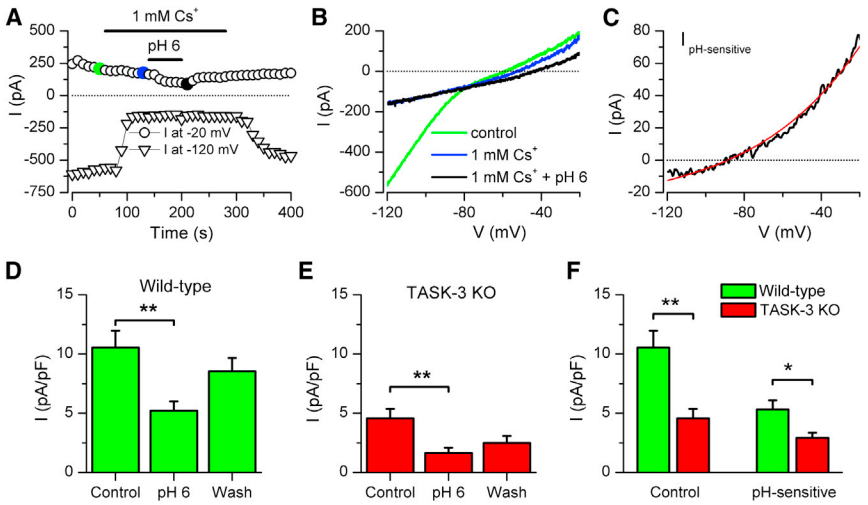

Figure 4. TRPM8 Neurons Express a TASK-3-like Current

(A) Time course of current at −20 and −120 mV during extracellular application of 1 mM Cs^+ and pH 6.0.

(B) Current ramps from −20 to −120 mV used to derive the data in (A). The colors of the traces correspond with the dots in (A).

(C) The pH-sensitive current obtained by digital subtraction of averages of three consecutive ramps at pH 7.4 and pH 6.0. The red line represents fitted values to a GHK equation that incorporates a pK/pNa ratio of 84.2 for this particular case.

(D) Histogram of mean ± SEM current density at −20 mV in control solution (pH 7.4), acidic solution (pH 6.0), and after wash in TRPM8 neurons of WT animals. Measurements were calculated in the presence of 1 mM external Cs^+ to block Ih current. **$p < 0.01$ ($n = 6$), one-way ANOVA and Dunnett's post hoc test.

(E) Same as in (D) but in TRPM8 neurons of TASK-3^{KO} mice ($n = 6$).

(F) Mean ± SEM current density at −20 mV in control solution (pH 7.4) and pH-sensitive current (current at pH 7.4 minus current at pH 6.0) in TRPM8 neurons of WT and TASK-3^{KO} animals. *$p < 0.05$ and **$p < 0.01$, unpaired t test.

5 mV in TASK-3^{KO} (−50 ± 2.0 mV, n = 16) compared to WT neurons (−54.6 ± 0.8 mV, n = 21; $p < 0.05$, unpaired t test). The electrophysiological characterization of TRPM8 neurons in WT and TASK-3^{KO} mice is summarized in Table 1. The overall excitability of the neurons was tested with an injection of depolarizing current pulses of increasing amplitude, after adjusting the membrane potential to −60 mV with direct current injection. As shown in Figure S7B, TASK-3^{KO} neurons fired more action potentials for the same depolarizing pulse, with a near-parallel displacement in the frequency-to-current (f-I) relationship. TASK-3^{KO} neurons also presented some alterations in the overall characteristics of the action potential, analyzed by phase plot analysis (Figures S7C–S7F). The main differences included a reduction in the amplitude of the action potential and the afterhyperpolarization (AHP), and a reduced rate of action potential repolarization in TASK-3^{KO} neurons ($p < 0.05$, unpaired t test). In contrast, action potential threshold was unchanged (−32.8 ± 0.7 mV in WT versus −31.3 ± 0.8 mV in TASK-3^{KO}; $p = 0.19$, unpaired t test). The rheobase and input resistance of TRPM8 neurons were not significantly affected in TASK-3^{KO} animals. Overall, these results indicate that TRPM8 neurons of TASK-3^{KO} mice are depolarized and have an enhanced electrical excitability, which can explain the increased cold sensitivity of these sensory neurons.

Cold Sensitivity Is Enhanced in TASK-3^{KO} Mice

Finally, we determined the consequences of TASK-3 deletion on cold perception in living mice. In a first series of behavioral experiments, we applied acetone to the hindpaws of WT and TASK-3^{KO} mice and measured the duration of licking and/or shaking of the paw that takes place in response to the evaporative cooling produced by the acetone. Compared to WT, TASK-3^{KO} mice responded to a drop of acetone in a most robust manner, but not to application of a drop of water at 37°C, a control for the mechanical stimuli associated with drop application (Figure 7A). This result suggested a greater sensitivity to cold in the TASK-3^{KO} mice. However, although this acetone test is a simple first-pass measure of cold sensitivity, it can also be associated with a distinct smell and possible chemical irritation. Thus, we tested the mice in a cold plantar assay (see Experimental Procedures) (Brenner et al., 2012). As a further validation for this method, we also tested the behavior of TRPM8^{KO} and TRPA1^{KO} mice. The paw withdrawal latency of TRPM8^{KO} mice exposed to dry ice nearly doubled compared to WT, going from 5.8 ± 0.3 s in WT ($n = 6$) to 9.8 ± 0.3 s in TRPM8^{KO} ($n = 9$; $p < 0.001$, one-way ANOVA and Bonferroni post hoc correction) (Figure 7B), consistent with the known severe deficit in cold sensing in these mice (Bautista et al., 2007; Dhaka et al., 2007). In contrast, withdrawal latency was unaffected in TRPA1^{KO} mice, in accordance with the modest role of TRPA1 in acute cold sensation in nonpathological conditions (Bautista et al., 2006; del Camino et al., 2010). Compared to WT, the withdrawal latency to the cold stimulus was significantly reduced in TASK-3^{KO} animals (4.5 ± 0.3 s in TASK-3^{KO}, $n = 11$; $p < 0.05$, one-way ANOVA). Using the calibration curve described in Experimental Procedures, we transformed the latencies into estimated temperatures at the plantar surface (Brenner et al., 2012). As shown in Figure 7C, the temperature withdrawal threshold was higher in TASK-3^{KO} (21.6°C ± 0.4°C) compared to WT (20.1°C ± 0.4°C; $p < 0.05$, one-way ANOVA).

DISCUSSION

Sensory neurons are morphologically and functionally diverse, and they have been traditionally classified by their responses to different stimuli and their electrical properties (Scott, 1992). This functional diversity is due in part to the distinct expression of transduction channels (reviewed by Abrahamsen et al., 2008; Belmonte

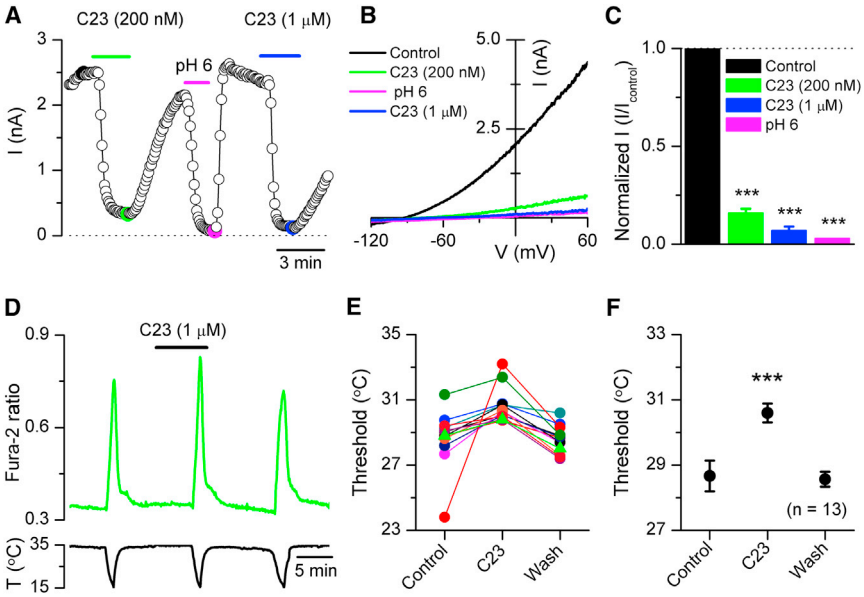

Figure 5. A Specific TASK-3 Antagonist Shifts the Temperature Threshold of TRPM8 Neurons

(A) Time course of current block caused by C23 and pH 6.0 on whole-cell currents at 0 mV in HEK293 cells transfected with mouse TASK-3. Currents were activated by 1 s duration voltage ramps from −120 to +60 mV at 33°C.

(B) Current-voltage relationship of whole-cell currents and the effects of C23 (200 nM and 1 μM) and pH 6.0. The corresponding current values at 0 mV are marked with large filled circles in (A).

(C) Summary histogram of the effects of C23 and pH 6.0 on whole-cell currents at 0 mV. C23 blocks TASK-3 currents: 84.0% ± 1.5% inhibition at 200 nM (n = 5) and 93.4% ± 1.6% inhibition at 1 μM (n = 4). pH 6.0 produced a 97.1% ± 0.3% inhibition (n = 5). Each response to C23 or pH 6.0 was normalized and compared to the preceding response in control solution. ***$p < 0.001$, paired t test.

(D) Time course of Fura-2 Ca^{2+} response in a $EYFP^+$ neuron challenged with three consecutive cooling pulses, before, during, and after exposure to C23 (1 μM).

(E) Effect of C23 (1 μM) on the cold-evoked threshold of 13 $EYFP^+$ neurons. The neuron depicted in (D) is represented by green triangles.

(F) Mean ± SEM effect of C23 on thermal threshold of $EYFP^+$ neurons. ***$p < 0.001$, paired t test.

and Viana, 2008). However, the current limited knowledge about specific markers for different populations of sensory neurons has complicated performing genomic-profiling studies on specific subpopulations. Here, we used a BAC genetic approach to label cold sensory neurons expressing the TRPM8 channel. The characterization of a $TRPM8^{BAC}$-$EYFP^{+/-}$ transgenic mouse line revealed that fluorescent-labeled neurons recapitulate the known cellular and functional properties of TRPM8 sensory neurons, including responses to cold and chemical agonists (McKemy et al., 2002; Peier et al., 2002a), effect of antagonists (Madrid et al., 2006), immunostaining profile (Dhaka et al., 2008; Takashima et al., 2007), and electrophysiological properties (Viana et al., 2002).

Ion Channel Profile of TRPM8-Expressing Neurons

We used this transgenic mouse line to establish the specific ion channel expression program for TRPM8 cold neurons. The reliability of our technique depends on the successful sorting of a pure population of TRPM8-expressing neurons. The fact that TRPM8 was enriched almost three orders of magnitude in EYFP-labeled neurons compared to unlabeled ones indicates that this was the case. Moreover, the pattern of ion channel expression in TRPM8 neurons was clearly distinct from that observed in a reference population composed of a mixture of sensory neurons, with some of the transcripts enriched >10-fold, indicating that absolute differences with other subpopulations included in the reference pool could be even larger. Ion channels visibly upregulated in TRPM8 neurons included some subunits previously implicated in cold transduction, such as TREK-1 (KCNK2) (Noël et al., 2009), or known to modulate their discharge pattern, like hyperpolarization-activated cyclic nucleotide-gated 1 (HCN1) channel (Orio et al., 2009), or their firing threshold, such as KCNQ2 (Vetter et al., 2013). However, we found enrichment of several additional transcripts, which are described below.

Like HCN1, HCN2 and HCN4 channels were also enriched in TRPM8 neurons, but HCN1 channel showed the highest absolute abundance. This is entirely consistent with the prominent expression of fast-activating Ih currents in cold thermoreceptors and their strong reduction in $HCN1^{KO}$ mice (Orio et al., 2009, 2012). The absolute levels of HCN4 were low (i.e., the expression is lower than for other members of the HCN family but differentially enriched in TRPM8-expressing neurons).

ASIC2, ASIC3, and ASIC4 showed relatively high levels in TRPM8 neurons. The function of ASIC channels in these neurons is currently unclear. However, it is noteworthy that ASIC channels are strongly modulated by cold temperatures (Askwith et al., 2001). Also, TRPM8 is strongly expressed in trigeminal terminals innervating taste buds (Figure S1B) (Abe et al., 2005), where ASICs are also strongly expressed. In fact, application of cold temperature to the tongue can evoke sour or salty taste perceptions (Cruz and Green, 2000). Moreover, cold activates many taste fibers, almost exclusively those responding to low pH and to salt (Lundy and Contreras, 1999). Thus, it is possible that ASICs and TRPM8 channels in gustatory and somatosensory afferents contribute to the processing of acidic and salty gustatory signals (Breza et al., 2006).

The expression of voltage-gated K^+ currents in DRG neurons is very diverse (Gold et al., 1996). We detected many subunits in TRPM8 neurons (Table S1). The fact that some of these subunits form functional heteromers increases the potential diversity even more. In the KCNC family, both KCNC18 (Kv3.1) and KCNC2 (Kv3.2) were significantly upregulated. These subunits are typical of fast-firing neurons with relatively little adaptation. Compared to other classes of somatosensory neurons, TRPM8 neurons are also fast firing and adapt only modestly to sustained depolarizations (Viana et al., 2002). A recent study identified

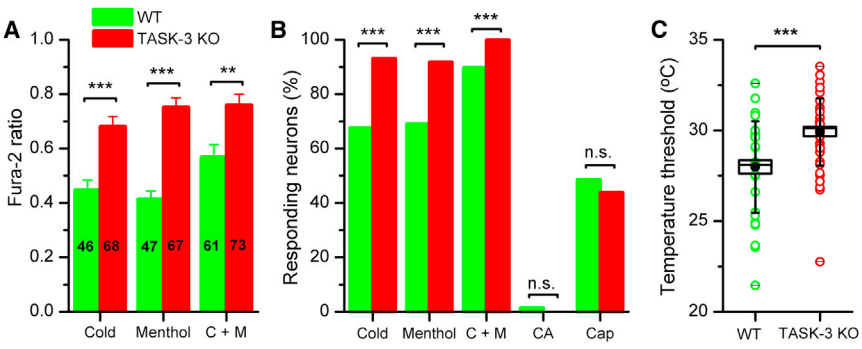

Figure 6. TASK-3 Modulates the Cold Sensitivity of TRPM8 Neurons

(A) Mean ± SEM Ca^{2+} elevation evoked by cold, menthol (100 μM), and cold (C) + menthol (M) in TRPM8(+) neurons in WT (green) and TASK-3^{KO} mice (red). **p < 0.01 and ***p < 0.001, unpaired t test.

(B) Percentage of TRPM8(+) neurons responding to different agonists in TASK-3^{WT} (green) and TASK-3^{KO} mice. CA (100 μM) and capsaicin (Cap; 100 nM) are shown.

(C) Temperature threshold of fluorescence-activated cell-sorted YFP^{+} neurons from $TRPM8^{BAC}$-$EYFP^{+/-}$ and $TRPM8^{BAC}$-$EYFP^{+/-}$; TASK-3^{KO} mice. ***p < 0.001, unpaired t test.

Kv3.1 in small DRG neurons, but their functional phenotype was not tested (Bocksteins et al., 2012).

In contrast, relative expression of some ion channels and receptor transcripts was reduced in TRPM8 neurons. For example, within the large family of Mrgprd receptors (>50 members), the 3 analyzed, belonging to 3 different subfamilies, were expressed at much lower levels in TRPM8 neurons. This result is consistent with their specific role as itch receptors and the lack of deficits in cold sensing after their selective ablation (Cavanaugh et al., 2009). In the case of Mrgprd, it is known to be expressed in a subpopulation of IB4-positive, nonpeptidergic mechanosensitive nociceptors (Dong et al., 2001). The low expression we found in TRPM8 neurons was also reported recently by in situ hybridization (Pogorzala et al., 2013).

High-threshold voltage-gated Ca^{2+} channels showed no clear differences in their expression when comparing TRPM8 neurons against the reference population. This is not entirely surprising, considering that all sensory neurons are engaged in synaptic transmission at the level of the dorsal horn. In the case of low-threshold, T-type Ca^{2+} current, mean levels were higher for the subunit α1G (Cav3.2) and lower for α1I (Cav3.3), although both levels were relatively low.

Differential Expression of TRP Channels in TRPM8 Neurons

With the exception of TRPV3 and TRPV4, two channels with poorly defined roles in thermosensation but activated by warm temperatures (Huang et al., 2011), the rest of TRP channels that we tested were detected in TRPM8 neurons (see Table S1). In the case of TRPV3, expression was not detected in the reference population either. This agrees with some previous findings that place TRPV3 in keratinocytes rather than in sensory neurons (Moqrich et al., 2005; Peier et al., 2002b). In contrast, TRPV4 was detected only in non-TRPM8 sensory neurons, albeit at low levels. In absolute values, the highest coexpression of TRPM8 was observed with TRPV1, although levels were only 60% of those obtained in the reference population. This colocalization is consistent with the immunocytochemical and functional results obtained by several laboratories, showing activation of about 50% of cold thermoreceptors by capsaicin (Dhaka et al., 2008; Reid et al., 2002; Viana et al., 2002). Expression of TRPA1 was very low in TRPM8 neurons, consistent with previous reports by Story et al. (2003) and Pogorzala et al. (2013).

We also found extensive expression of TRPC3, TRPC5, and TRPC6 within DRGs, which are mechano-gated TRP channels (Gomis et al., 2008; Quick et al., 2012). Consistent with previous studies that suggested their broad expression within DRGs but with a preferential expression in IB4-positive, nonpeptidergic neurons (Elg et al., 2007; Quick et al., 2012; Vandewauw et al., 2013), we found that the expression of these channels was substantially lower in TRPM8 neurons compared with the rest of neurons. In agreement with this finding, the behavioral phenotype of TRPC6-TRPC3 ablation is a selective deficit in innocuous mechanosensitivity (Quick et al., 2012). TRPC2 was the only TRPC channel enriched in TRPM8 neurons, although it showed modest absolute levels. Transcripts for this channel were detected previously in DRG, but its function, outside the vomeronasal system, has not been characterized yet (Elg et al., 2007).

Role of TASK-3 K^{+} Channels in Cold Temperature Transduction

Our work reveals that the TASK-3 is highly expressed in a subpopulation of TRPM8 cold-sensitive neurons. Interestingly, other members of the K2P channel family (TREK-1, TREK-2, and TRAAK) are very sensitive to temperature (Kang et al., 2005; Maingret et al., 2000) and have been shown to play important roles in modulating the excitability of sensory neurons, including nociceptors (Acosta et al., 2014; Noël et al., 2009). Relative to other K2P channels, TASK-3 shows low-expression values in rat DRG at the level of the whole ganglia (Marsh et al., 2012). However, previous in situ hybridization data showed that TASK-3 expression is restricted to a very small subpopulation of DRG neurons (Talley et al., 2001). This would be consistent with a selective expression in a fraction of TRPM8 neurons, which represent a small percentage of all DRG neurons (McKemy et al., 2002; Peier et al., 2002a). Again, this result emphasizes the importance of characterizing expression levels in specific subsets of functionally homogeneous neurons to reach valid conclusions regarding their functional roles. We find that in the absence of TASK-3, TRPM8 neurons increased their sensitivity to cold temperature very markedly. Also, a blocker of TASK-3 shifted the cold threshold of TRPM8 neurons to warmer temperatures. Moreover, cold-sensitive neurons in TASK-3^{KO} mice were depolarized and fired more action potentials during a depolarizing current pulse. The excitability increase in vivo is probably larger than measured electrophysiologically because

Table 1. Electrophysiological Properties of TRPM8$^+$ DRG Neurons in WT and TASK-3^{KO} Mice

	WT (n = 21)	TASK-3^{KO} (n = 16)	p Value
RMP (mV)	−54.6 ± 0.8	−50 ± 2.0	<0.05
AP threshold (mV)	−32.8 ± 0.7	−31.4 ± 0.8	0.19
AP overshoot (mV)	33.82 ± 1.27	33.82 ± 1.27	0.24
AP amplitude (mV)	104.7 ± 1.2	97.4 ± 1.9	<0.001
AP duration (ms)	1.12 ± 0.02	1.20 ± 0.05	0.24
AP depolarization rate (mV/ms)	314 ± 5	268 ± 23	0.11
AP repolarization rate (mV/ms)	−104 ± 5	−84 ± 6	<0.05
AHP peak (mV)	−71.1 ± 0.8	−66.2 ± 1.1	<0.001
Input resistance (MΩ)	857 ± 65	971 ± 90	0.30
Rheobase current (pA)	22.9 ± 1.6	22.5 ± 1.7	0.88
Sag ratio (%)	0.78 ± 0.02	0.73 ± 0.02	0.07

All recordings were performed in perforated whole-cell current-clamp mode. After determining the resting membrane potential (RMP), the potential was adjusted to −60 mV. Action potential (AP) overshoot is the absolute peak voltage value from 0 mV. AP amplitude is measured from the overshoot peak to the most negative voltage reached during the AHP immediately after the AP. AP duration is measured at half-maximal amplitude. The sag ratio, a measure of the Ih, was assessed from the amplitude ratio of the voltage at peak and at steady state during a 150 ms hyperpolarizing current pulse of −120 pA. All statistical comparisons were performed with an unpaired t test.

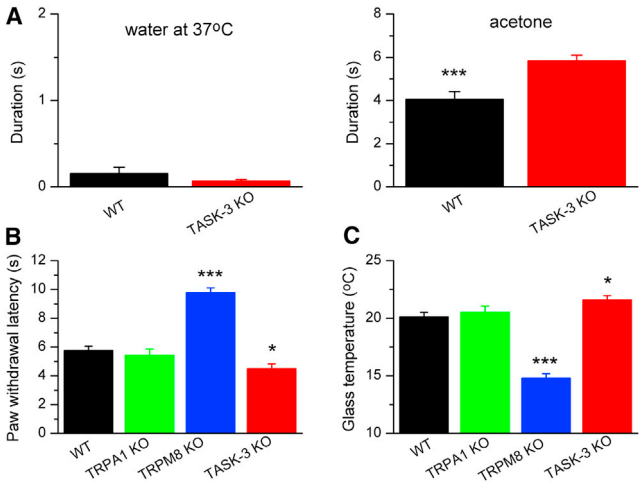

Figure 7. Cold Sensitivity Is Augmented in TASK-3^{KO} Mice

(A) Duration of behavior (lift, shake, lick) to application of a drop of water (left) or acetone in male WT (n = 15) or TASK-3^{KO} mice (n = 16). ***p < 0.001, unpaired t test.

(B) Paw withdrawal latency to application of a dry ice pellet to the bottom face of a glass plate in male WT (n = 6), TRPA1 KO (n = 9), TRPM8 KO (n = 9), and TASK-3^{KO} mice (n = 11). *p < 0.05 and ***p < 0.001, one-way ANOVA and Bonferroni posttest.

(C) Estimated temperature at the skin surface in the same experiment as in (B). *p < 0.05 and ***p < 0.001, one-way ANOVA and Bonferroni posttest.

we corrected the strong depolarization for comparison purposes. TRPM8 sensory neurons exhibit different temperature thresholds (Babes et al., 2004; Madrid et al., 2009; Nealen et al., 2003) and participate in the detection of innocuous and noxious cold signals (Knowlton et al., 2010, 2013). Importantly, the population of high-threshold cold-sensitive neurons (activated below 26.5°C) was almost absent in the TASK-3^{KO} mice, suggesting a role for this channel in setting the threshold of cold thermoreceptors. Finally, we also show that deletion of TASK-3 resulted in behavioral changes in cold sensitivity in vivo. These changes were moderate, which is not entirely surprising considering that TASK-3 is expressed in only about one-third of all TRPM8$^+$ neurons. Moreover, the possible coexpression of other leak K^+ channels may compensate the deficit of TASK-3.

A previous study reported that TASK-1 and TASK-3 channels are reduced during inflammation, and this reduction was correlated with the appearance of signs of spontaneous pain (Marsh et al., 2012), suggesting that changes in the expression of TASK-1–TASK-3, and other K2P channels, play a role in the manifestation of different pain modalities. From our results, it is logical to postulate that downregulation of TASK-3 in TRPM8 cold neurons could be involved in the development of cold hypersensitivity during inflammatory and/or neuropathic conditions (Choi et al., 1994). Future studies should examine this hypothesis.

In summary, we present a detailed ion channel expression profile of TRPM8$^+$ peripheral cold thermoreceptors. We identify several ion channels enriched in these primary sensory neurons. Importantly, we reveal a role for TASK-3 leak K^+ channels in cold sensitivity, a functional role missed for years even though other members of K2P family channels had been already implicated in thermosensation. The expression of TASK-3 modulates the excitability of TRPM8 cold thermoreceptors and participates in the specification of the high-threshold subpopulation of TRPM8 sensory neurons. This approach opens possibilities for the molecular profiling and functional characterization, not only of cold thermoreceptors, but for other sensory submodalities as well. We envision that this strategy will help establish changes in expression levels of particular ion channels in specific subpopulations of injured sensory neurons, identifying potential therapeutic targets for pain treatment.

EXPERIMENTAL PROCEDURES

Detailed information of the Experimental Procedures is available in the Supplemental Experimental Procedures.

Animals

Animal experiments were performed in accordance with the guidelines established by the European Communities Council Directive (86/609/ECC), by Spanish Royal Decree 1201/2005, and the Animal Care and Use Guidelines from the NIH. Animal protocols were approved by the Animal Care Committee of the Universidad Miguel Hernández and the Animal Care and Use Committee of the University of Virginia. The TASK-3^{KO} mice were previously described by Mulkey et al. (2007).

Genetic Labeling of TRPM8-Expressing Cold Sensory Neurons

Specific labeling of TRPM8-expressing neurons with YFP was achieved by BAC recombineering (Gong et al., 2002), using BAC RP24-78N24 (Children's Hospital Oakland Research Institute, BACPAC Resources Center) containing

the entire locus of TRPM8 gene plus 108.6 kb upstream and 52 kb downstream flanking regions. Eight different founders were identified. All experiments were performed on line CM1. F2 offspring were obtained to study germline transmission. Correct EYFP expression in DRG, TG, and spinal cord was confirmed in all lines obtained.

FACS and mRNA Quantification

Following enzymatic dissociation, labeled DRG neurons were purified by FACS using a FACSAria III (BD Biosciences). The quantity and purity of sorted cells were verified by fluorescent microscopy. Custom-designed TaqMan low-density array plates (96 wells) (Micro Fluidic Cards; Applied Biosystems) were used to quantify relative mRNA expression in TRPM8 neurons. Samples from fluorescent and nonfluorescent cells were collected and analyzed simultaneously, using the threshold cycle relative quantification method.

Electrophysiology and Ca^{2+} Imaging of DRG Neurons

Electrophysiological and Ca^{2+}-imaging experiments were performed on primary cultures of TRPM8-expressing DRG neurons of WT and TASK-3^{KO} mice, following procedures described elsewhere by Madrid et al. (2009). Whole-cell voltage and perforated current-clamp recordings were performed at a temperature of 32°C–34°C with a MultiClamp 700B amplifier (Molecular Devices). Basic electrophysiological properties (input resistance, rheobase current, spike duration, inward rectification, and frequency-current relationships) and quantitative characteristics of the action potential were analyzed in current-clamp mode. For analysis of the pH-sensitive current (I_{pH}), the currents obtained at pH 7.4 and pH 6.0 were digitally subtracted, and the resulting I–V curves were fitted with a standard GHK current equation that included Na^+ and K^+ permeability terms.

Behavioral Testing of Cold Sensitivity

Behavioral testing of cold sensitivity in adult male mice followed the method of Brenner, based on the withdrawal latency to the application of a pellet of dry ice to the glass surface where the animals rest (Brenner et al., 2012).

Drugs

1-{1-[6-(biphenyl-4-ylcarbonyl)-5,6,7,8-tetrahydropyrido[4,3-d]-pyrimidin-4-yl]piperidin-4-yl} (propan-1-one) (C23) was a kind gift of Merck. BCTC was purchased from Tocris, l-menthol was purchased from Scharlau Chemie, and cesium chloride and zinc chloride were from Sigma-Aldrich.

Statistical Analysis

Unless stated otherwise, data are reported as mean ± SEM. Statistical significance ($p < 0.05$) was assessed by Student's t test. Paired tests were applied when appropriate. For multiple group comparisons, a one-way ANOVA test was used.

SUPPLEMENTAL INFORMATION

Supplemental Information includes Supplemental Experimental Procedures, seven figures, and two tables and can be found with this article online at http://dx.doi.org/10.1016/j.celrep.2014.08.003.

AUTHOR CONTRIBUTIONS

C.M.-P. and F.V. designed the project. C.M.-P. generated the TRPM8 transgenic lines and performed all histological, biochemical, and molecular experiments. E.L. performed electrophysiological and calcium imaging experiments. E.Q. assisted with animal genotyping and FACS experiments. C.F.-P. and J.L.W. performed behavioral experiments. D.A.B. designed and supervised the generation of TASK-3^{KO} mice. C.M.-P., D.A.B., and F.V. wrote the manuscript.

ACKNOWLEDGMENTS

The authors are grateful to Hugo Cabedo, Laura Almaraz, Eloisa Herrera, and Vincent Santarelli for comments and Carlos Belmonte for financial support. They thank Mark Zylka for helpful advice on FACS techniques and Pilar Cidad and María Teresa Pérez García for advice on TaqMan array methodology. We thank Merck & Co. for generously providing Compound 23. C.M.-P. was a JAE postdoctoral fellow; E.L. and C.F.-P. held predoctoral fellowships from the Generalitat Valenciana (GRISOLIA/2008/025). Funding was provided by NIH (NS33583 to D.A.B.), Spanish MINECO SAF2010-14990 and SAF2013-45608-R and Prometeo/2014/011 from Generalitat Valenciana (to F.V.), and CONSOLIDER-INGENIO 2010 CSD2007-0002 (to Carlos Belmonte). The Instituto de Neurociencias de Alicante is a "Centre of Excellence Severo Ochoa."

Received: February 25, 2014
Revised: June 9, 2014
Accepted: August 1, 2014
Published: September 4, 2014

REFERENCES

Abe, J., Hosokawa, H., Okazawa, M., Kandachi, M., Sawada, Y., Yamanaka, K., Matsumura, K., and Kobayashi, S. (2005). TRPM8 protein localization in trigeminal ganglion and taste papillae. Brain Res. Mol. Brain Res. *136*, 91–98.

Abrahamsen, B., Zhao, J., Asante, C.O., Cendan, C.M., Marsh, S., Martinez-Barbera, J.P., Nassar, M.A., Dickenson, A.H., and Wood, J.N. (2008). The cell and molecular basis of mechanical, cold, and inflammatory pain. Science *321*, 702–705.

Acosta, C., Djouhri, L., Watkins, R., Berry, C., Bromage, K., and Lawson, S.N. (2014). TREK2 expressed selectively in IB4-binding C-fiber nociceptors hyperpolarizes their membrane potentials and limits spontaneous pain. J. Neurosci. *34*, 1494–1509.

Almaraz, L., Manenschijn, J.A., de la Peña, E., and Viana, F. (2014). Trpm8. Handbook Exp. Pharmacol. *222*, 547–579.

Andersson, D.A., Gentry, C., Moss, S., and Bevan, S. (2009). Clioquinol and pyrithione activate TRPA1 by increasing intracellular Zn2+. Proc. Natl. Acad. Sci. USA *106*, 8374–8379.

Askwith, C.C., Benson, C.J., Welsh, M.J., and Snyder, P.M. (2001). DEG/ENaC ion channels involved in sensory transduction are modulated by cold temperature. Proc. Natl. Acad. Sci. USA *98*, 6459–6463.

Babes, A., Zorzon, D., and Reid, G. (2004). Two populations of cold-sensitive neurons in rat dorsal root ganglia and their modulation by nerve growth factor. Eur. J. Neurosci. *20*, 2276–2282.

Bandell, M., Macpherson, L.J., and Patapoutian, A. (2007). From chills to chilis: mechanisms for thermosensation and chemesthesis via thermoTRPs. Curr. Opin. Neurobiol. *17*, 490–497.

Bautista, D.M., Jordt, S.E., Nikai, T., Tsuruda, P.R., Read, A.J., Poblete, J., Yamoah, E.N., Basbaum, A.I., and Julius, D. (2006). TRPA1 mediates the inflammatory actions of environmental irritants and proalgesic agents. Cell *124*, 1269–1282.

Bautista, D.M., Siemens, J., Glazer, J.M., Tsuruda, P.R., Basbaum, A.I., Stucky, C.L., Jordt, S.E., and Julius, D. (2007). The menthol receptor TRPM8 is the principal detector of environmental cold. Nature *448*, 204–208.

Belmonte, C., and Viana, F. (2008). Molecular and cellular limits to somatosensory specificity. Mol. Pain *4*, 14.

Belmonte, C., Brock, J.A., and Viana, F. (2009). Converting cold into pain. Exp. Brain Res. *196*, 13–30.

Bocksteins, E., Van de Vijver, G., Van Bogaert, P.P., and Snyders, D.J. (2012). Kv3 channels contribute to the delayed rectifier current in small cultured mouse dorsal root ganglion neurons. Am. J. Physiol. Cell Physiol. *303*, C406–C415.

Brenner, D.S., Golden, J.P., and Gereau, R.W., 4th. (2012). A novel behavioral assay for measuring cold sensation in mice. PLoS One *7*, e39765.

Breza, J.M., Curtis, K.S., and Contreras, R.J. (2006). Temperature modulates taste responsiveness and stimulates gustatory neurons in the rat geniculate ganglion. J. Neurophysiol. *95*, 674–685.

Cavanaugh, D.J., Lee, H., Lo, L., Shields, S.D., Zylka, M.J., Basbaum, A.I., and Anderson, D.J. (2009). Distinct subsets of unmyelinated primary sensory fibers

mediate behavioral responses to noxious thermal and mechanical stimuli. Proc. Natl. Acad. Sci. USA *106*, 9075–9080.

Choi, Y., Yoon, Y.W., Na, H.S., Kim, S.H., and Chung, J.M. (1994). Behavioral signs of ongoing pain and cold allodynia in a rat model of neuropathic pain. Pain *59*, 369–376.

Clapham, D.E. (2003). TRP channels as cellular sensors. Nature *426*, 517–524.

Clarke, C.E., Veale, E.L., Green, P.J., Meadows, H.J., and Mathie, A. (2004). Selective block of the human 2-P domain potassium channel, TASK-3, and the native leak potassium current, IKSO, by zinc. J. Physiol. *560*, 51–62.

Coburn, C.A., Luo, Y., Cui, M., Wang, J., Soll, R., Dong, J., Hu, B., Lyon, M.A., Santarelli, V.P., Kraus, R.L., et al. (2012). Discovery of a pharmacologically active antagonist of the two-pore-domain potassium channel K2P9.1 (TASK-3). ChemMedChem *7*, 123–133.

Colburn, R.W., Lubin, M.L., Stone, D.J., Jr., Wang, Y., Lawrence, D., D'Andrea, M.R., Brandt, M.R., Liu, Y., Flores, C.M., and Qin, N. (2007). Attenuated cold sensitivity in TRPM8 null mice. Neuron *54*, 379–386.

Cruz, A., and Green, B.G. (2000). Thermal stimulation of taste. Nature *403*, 889–892.

de la Peña, E., Mälkiä, A., Vara, H., Caires, R., Ballesta, J.J., Belmonte, C., and Viana, F. (2012). The influence of cold temperature on cellular excitability of hippocampal networks. PLoS One *7*, e52475.

del Camino, D., Murphy, S., Heiry, M., Barrett, L.B., Earley, T.J., Cook, C.A., Petrus, M.J., Zhao, M., D'Amours, M., Deering, N., et al. (2010). TRPA1 contributes to cold hypersensitivity. J. Neurosci. *30*, 15165–15174.

Dhaka, A., Murray, A.N., Mathur, J., Earley, T.J., Petrus, M.J., and Patapoutian, A. (2007). TRPM8 is required for cold sensation in mice. Neuron *54*, 371–378.

Dhaka, A., Earley, T.J., Watson, J., and Patapoutian, A. (2008). Visualizing cold spots: TRPM8-expressing sensory neurons and their projections. J. Neurosci. *28*, 566–575.

Dong, X., Han, S., Zylka, M.J., Simon, M.I., and Anderson, D.J. (2001). A diverse family of GPCRs expressed in specific subsets of nociceptive sensory neurons. Cell *106*, 619–632.

Duprat, F., Lesage, F., Fink, M., Reyes, R., Heurteaux, C., and Lazdunski, M. (1997). TASK, a human background K+ channel to sense external pH variations near physiological pH. EMBO J. *16*, 5464–5471.

Elg, S., Marmigere, F., Mattsson, J.P., and Ernfors, P. (2007). Cellular subtype distribution and developmental regulation of TRPC channel members in the mouse dorsal root ganglion. J. Comp. Neurol. *503*, 35–46.

Foulkes, T., and Wood, J.N. (2007). Mechanisms of cold pain. Channels (Austin) *1*, 154–160.

Gold, M.S., Shuster, M.J., and Levine, J.D. (1996). Characterization of six voltage-gated K+ currents in adult rat sensory neurons. J. Neurophysiol. *75*, 2629–2646.

Gomis, A., Soriano, S., Belmonte, C., and Viana, F. (2008). Hypoosmotic- and pressure-induced membrane stretch activate TRPC5 channels. J. Physiol. *586*, 5633–5649.

Gong, S., Yang, X.W., Li, C., and Heintz, N. (2002). Highly efficient modification of bacterial artificial chromosomes (BACs) using novel shuttle vectors containing the R6Kgamma origin of replication. Genome Res. *12*, 1992–1998.

Hu, H., Bandell, M., Petrus, M.J., Zhu, M.X., and Patapoutian, A. (2009). Zinc activates damage-sensing TRPA1 ion channels. Nat. Chem. Biol. *5*, 183–190.

Huang, S.M., Li, X., Yu, Y., Wang, J., and Caterina, M.J. (2011). TRPV3 and TRPV4 ion channels are not major contributors to mouse heat sensation. Mol. Pain *7*, 37.

Julius, D. (2013). TRP channels and pain. Annu. Rev. Cell Dev. Biol. *29*, 355–384.

Kang, D., Choe, C., and Kim, D. (2005). Thermosensitivity of the two-pore domain K+ channels TREK-2 and TRAAK. J. Physiol. *564*, 103–116.

Kim, Y., Bang, H., and Kim, D. (2000). TASK-3, a new member of the tandem pore K(+) channel family. J. Biol. Chem. *275*, 9340–9347.

Knowlton, W.M., Bifolck-Fisher, A., Bautista, D.M., and McKemy, D.D. (2010). TRPM8, but not TRPA1, is required for neural and behavioral responses to acute noxious cold temperatures and cold-mimetics in vivo. Pain *150*, 340–350.

Knowlton, W.M., Palkar, R., Lippoldt, E.K., McCoy, D.D., Baluch, F., Chen, J., and McKemy, D.D. (2013). A sensory-labeled line for cold: TRPM8-expressing sensory neurons define the cellular basis for cold, cold pain, and cooling-mediated analgesia. J. Neurosci. *33*, 2837–2848.

Lesage, F., and Barhanin, J. (2011). Molecular physiology of pH-sensitive background K(2P) channels. Physiology (Bethesda) *26*, 424–437.

Lumpkin, E.A., and Caterina, M.J. (2007). Mechanisms of sensory transduction in the skin. Nature *445*, 858–865.

Lundy, R.F., Jr., and Contreras, R.J. (1999). Gustatory neuron types in rat geniculate ganglion. J. Neurophysiol. *82*, 2970–2988.

Ma, Q. (2010). Labeled lines meet and talk: population coding of somatic sensations. J. Clin. Invest. *120*, 3773–3778.

Madrid, R., Donovan-Rodríguez, T., Meseguer, V., Acosta, M.C., Belmonte, C., and Viana, F. (2006). Contribution of TRPM8 channels to cold transduction in primary sensory neurons and peripheral nerve terminals. J. Neurosci. *26*, 12512–12525.

Madrid, R., de la Peña, E., Donovan-Rodriguez, T., Belmonte, C., and Viana, F. (2009). Variable threshold of trigeminal cold-thermosensitive neurons is determined by a balance between TRPM8 and Kv1 potassium channels. J. Neurosci. *29*, 3120–3131.

Maingret, F., Lauritzen, I., Patel, A.J., Heurteaux, C., Reyes, R., Lesage, F., Lazdunski, M., and Honoré, E. (2000). TREK-1 is a heat-activated background K(+) channel. EMBO J. *19*, 2483–2491.

Marsh, B., Acosta, C., Djouhri, L., and Lawson, S.N. (2012). Leak K^+ channel mRNAs in dorsal root ganglia: relation to inflammation and spontaneous pain behaviour. Mol. Cell. Neurosci. *49*, 375–386.

McKemy, D.D., Neuhausser, W.M., and Julius, D. (2002). Identification of a cold receptor reveals a general role for TRP channels in thermosensation. Nature *416*, 52–58.

Moqrich, A., Hwang, S.W., Earley, T.J., Petrus, M.J., Murray, A.N., Spencer, K.S., Andahazy, M., Story, G.M., and Patapoutian, A. (2005). Impaired thermosensation in mice lacking TRPV3, a heat and camphor sensor in the skin. Science *307*, 1468–1472.

Mulkey, D.K., Talley, E.M., Stornetta, R.L., Siegel, A.R., West, G.H., Chen, X., Sen, N., Mistry, A.M., Guyenet, P.G., and Bayliss, D.A. (2007). TASK channels determine pH sensitivity in select respiratory neurons but do not contribute to central respiratory chemosensitivity. J. Neurosci. *27*, 14049–14058.

Nealen, M.L., Gold, M.S., Thut, P.D., and Caterina, M.J. (2003). TRPM8 mRNA is expressed in a subset of cold-responsive trigeminal neurons from rat. J. Neurophysiol. *90*, 515–520.

Noël, J., Zimmermann, K., Busserolles, J., Deval, E., Alloui, A., Diochot, S., Guy, N., Borsotto, M., Reeh, P., Eschalier, A., and Lazdunski, M. (2009). The mechano-activated K+ channels TRAAK and TREK-1 control both warm and cold perception. EMBO J. *28*, 1308–1318.

Orio, P., Madrid, R., de la Peña, E., Parra, A., Meseguer, V., Bayliss, D.A., Belmonte, C., and Viana, F. (2009). Characteristics and physiological role of hyperpolarization activated currents in mouse cold thermoreceptors. J. Physiol. *587*, 1961–1976.

Orio, P., Parra, A., Madrid, R., González, O., Belmonte, C., and Viana, F. (2012). Role of Ih in the firing pattern of mammalian cold thermoreceptor endings. J. Neurophysiol. *108*, 3009–3023.

Parra, A., Madrid, R., Echevarria, D., del Olmo, S., Morenilla-Palao, C., Acosta, M.C., Gallar, J., Dhaka, A., Viana, F., and Belmonte, C. (2010). Ocular surface wetness is regulated by TRPM8-dependent cold thermoreceptors of the cornea. Nat. Med. *16*, 1396–1399.

Peier, A.M., Moqrich, A., Hergarden, A.C., Reeve, A.J., Andersson, D.A., Story, G.M., Earley, T.J., Dragoni, I., McIntyre, P., Bevan, S., and Patapoutian, A. (2002a). A TRP channel that senses cold stimuli and menthol. Cell *108*, 705–715.

Peier, A.M., Reeve, A.J., Andersson, D.A., Moqrich, A., Earley, T.J., Hergarden, A.C., Story, G.M., Colley, S., Hogenesch, J.B., McIntyre, P., et al.

(2002b). A heat-sensitive TRP channel expressed in keratinocytes. Science *296*, 2046–2049.

Plant, L.D. (2012). A role for K2P channels in the operation of somatosensory nociceptors. Front Mol Neurosci *5*, 21.

Pogorzala, L.A., Mishra, S.K., and Hoon, M.A. (2013). The cellular code for mammalian thermosensation. J. Neurosci. *33*, 5533–5541.

Quick, K., Zhao, J., Eijkelkamp, N., Linley, J.E., Rugiero, F., Cox, J.J., Raouf, R., Gringhuis, M., Sexton, J.E., Abramowitz, J., et al. (2012). TRPC3 and TRPC6 are essential for normal mechanotransduction in subsets of sensory neurons and cochlear hair cells. Open Biol *2*, 120068.

Reid, G., and Flonta, M. (2001). Cold transduction by inhibition of a background potassium conductance in rat primary sensory neurones. Neurosci. Lett. *297*, 171–174.

Reid, G., Babes, A., and Pluteanu, F. (2002). A cold- and menthol-activated current in rat dorsal root ganglion neurones: properties and role in cold transduction. J. Physiol. *545*, 595–614.

Scott, S.A. (1992). Sensory Neurons: Diversity, Development, and Plasticity (New York: Oxford University Press).

Story, G.M., Peier, A.M., Reeve, A.J., Eid, S.R., Mosbacher, J., Hricik, T.R., Earley, T.J., Hergarden, A.C., Andersson, D.A., Hwang, S.W., et al. (2003). ANKTM1, a TRP-like channel expressed in nociceptive neurons, is activated by cold temperatures. Cell *112*, 819–829.

Takashima, Y., Daniels, R.L., Knowlton, W., Teng, J., Liman, E.R., and McKemy, D.D. (2007). Diversity in the neural circuitry of cold sensing revealed by genetic axonal labeling of transient receptor potential melastatin 8 neurons. J. Neurosci. *27*, 14147–14157.

Talley, E.M., and Bayliss, D.A. (2002). Modulation of TASK-1 (Kcnk3) and TASK-3 (Kcnk9) potassium channels: volatile anesthetics and neurotransmitters share a molecular site of action. J. Biol. Chem. *277*, 17733–17742.

Talley, E.M., Solorzano, G., Lei, Q., Kim, D., and Bayliss, D.A. (2001). Cns distribution of members of the two-pore-domain (KCNK) potassium channel family. J. Neurosci. *21*, 7491–7505.

Vandewauw, I., Owsianik, G., and Voets, T. (2013). Systematic and quantitative mRNA expression analysis of TRP channel genes at the single trigeminal and dorsal root ganglion level in mouse. BMC Neurosci. *14*, 21.

Vetter, I., Hein, A., Sattler, S., Hessler, S., Touska, F., Bressan, E., Parra, A., Hager, U., Leffler, A., Boukalova, S., et al. (2013). Amplified cold transduction in native nociceptors by M-channel inhibition. J. Neurosci. *33*, 16627–16641.

Viana, F., de la Peña, E., and Belmonte, C. (2002). Specificity of cold thermotransduction is determined by differential ionic channel expression. Nat. Neurosci. *5*, 254–260.

Xing, H., Ling, J., Chen, M., and Gu, J.G. (2006). Chemical and cold sensitivity of two distinct populations of TRPM8-expressing somatosensory neurons. J. Neurophysiol. *95*, 1221–1230.